Fusion of *KIF5B* and *RET* transforming gene in lung adenocarcinoma revealed from whole-genome and transcriptome sequencing

Young Seok Ju, Won-Chul Lee, Jong-Yeon Shin, et al.

Genome Res. published online December 22, 2011
Access the most recent version at doi:10.1101/gr.133645.111

Fusion of *KIF5B* and *RET* transforming gene in lung adenocarcinoma revealed from whole-genome and transcriptome sequencing

Author list

Young Seok Ju[1,2], Won-Chul Lee[1,3], Jong-Yeon Shin[1,4], Seungbok Lee[1,3], Thomas Bleazard[1], Jae-Kyung Won[5], Young Tae Kim[6,7], Jong-Il Kim[1,3,4,8], Jin-Hyoung Kang[9] and Jeong-Sun Seo[1,2,3,4,8]

Affiliation

1. Genomic Medicine Institute (GMI), Medical Research Center, Seoul National University, Seoul 110-799, Korea
2. Macrogen Inc., Seoul 153-781, Korea
3. Department of Biomedical Sciences, Seoul National University Graduate School, Seoul 110-799, Korea
4. Psoma Therapeutics Inc., Seoul, 153-781, Korea
5. Molecular Pathology Center, Seoul National University Cancer Hospital, Seoul 110-744, Korea
6. Department of Thoracic and Cardiovascular Surgery, Clinical Research Institute, Seoul National University Hospital, Seoul 110-799, Korea
7. Cancer Research Institute, Seoul National University College of Medicine, Seoul 110-799, Korea
8. Department of Biochemistry and Molecular Biology, Seoul National University College of Medicine, Seoul 110-799, Korea
9. Department of Internal Medicine, Seoul St. Mary's Hospital, The Catholic University, Seoul 137-040, Korea

Corresponding Author

To whom correspondence should be addressed;

Jeong-Sun Seo, M.D., Ph.D.

Genomic Medicine Institute, Medical Research Center,
Department of Biochemistry and Molecular Biology, Seoul National University College of Medicine
28 Yongon-Dong, Jongno-Gu, Seoul 110-799, Korea
Phone: 82-2-740-8246
Fax: 82-2-741-5423
E-mail: jeongsun@snu.ac.kr

Abstract

Identification of the molecular events which drive cancer transformation is essential to the development of targeted agents which improve the clinical outcome of lung cancer. Many studies have reported genomic driver mutations in non-small cell lung cancers (NSCLC) over the past decade, however, the molecular pathogenesis of more than 40% of NSCLC is still unknown. To identify new molecular targets in NSCLC, we performed the combined analysis of massively parallel whole-genome and transcriptome sequencing for cancer and paired normal tissue of a 33-year-old lung adenocarcinoma patient, who is a never-smoker and has no familial cancer history. The cancer showed no known driver mutation in *EGFR* or *KRAS* and no *EML4-ALK* fusion. Here we report a novel fusion gene between *KIF5B* and *RET* proto-oncogene caused by a pericentric inversion of 10p11.22-q11.21. This fusion gene overexpresses chimeric RET receptor tyrosine kinase, which could spontaneously induce cellular transformation. We identified the *KIF5B-RET* fusion in two more cases out of twenty primary lung adenocarcinomas in the replication study. Our data demonstrate that a subset of NSCLC could be caused by a fusion of *KIF5B* and *RET*, and suggest the chimeric oncogene as a promising molecular target for the personalized diagnosis and treatment of lung cancer.

Introduction

Lung cancer remains a leading cause of mortality in cancer, with around 1.38 million deaths worldwide annually (Ferlay et al. 2010). With conventional chemotherapeutic regimen, the median survival time for lung cancer patients in advanced stages is less than one year from diagnosis (Schiller et al. 2002). Tobacco smoking is known to be a major risk factor of lung cancer in Western countries, where 85% to 90% of all lung cancers were attributed to smoking (Toh et al. 2006). However, approximately 25% of lung cancer patients worldwide are 'never-smokers' (Lee et al. 2011). Data from many Asian countries have shown that 'never-smokers' constitute 30-40% of non-small-cell lung cancer (NSCLC). NSCLC accounts for ~80% of lung cancer cases (Subramanian and Govindan 2007), and the dominant histological type is adenocarcinoma (>50%) (Pao and Girard 2011).

Lung cancer of never-smokers tends to be driven by single somatic mutation events, rather than global genetic and epigenetic changes (Lee et al. 2011). A subset of somatic mutations has been reported in NSCLC in the past few years, such as *EGFR*, *KRAS and EML4-ALK* genes (which are conventionally called 'the triple-markers') (Pao and Girard 2011). Mutations in the tyrosine kinase domain of *EGFR*, which are associated preferentially with NSCLC of non-smokers and Asians, are sensitive to *EGFR* targeted therapy, such as gefitinib (Paez et al. 2004). Missense mutations in *KRAS* are common in the lung adenocarcinomas of smokers, and induce resistance to *EGFR* inhibitors (Riely et al. 2008). More recently, the *EML4-ALK* fusion gene was identified in NSCLC (Soda et al. 2007), which is generated by inversion in chromosome 2. This fusion gene, formed by chromosomal rearrangement, is more frequently detected in lung adenocarcinoma of young patients, regardless of ethnicity, with no or little history of cigarette smoking (Wong et al. 2009). *ALK* positive lung cancer constitutes ~5% of NSCLC, and is highly sensitive to *ALK* inhibitors, such as crizotinib (Pao and Girard 2011).

Although several genetic mutations have been reported previously, a large proportion of lung cancer patients have been observed to have none of them in their cancer genome. More than 40% of NSCLC appear to be driven by unknown genetic events (Harris 2010; Pao and Girard 2011).

Here we report a novel fusion gene generated by a chromosomal inversion event in a young, never-smoker lung adenocarcinoma patient, whose cancer was negative for the triple-markers, using massively parallel DNA and RNA sequencing. The patient, known as AK55, was healthy until 33 years of age, when a poorly differentiated adenocarcinoma developed in the right upper lobe of lung (Figure 1A). He has no known family history of cancers from grandparents and he is a never-smoker. Metastases in liver and multiple bones were also detected in PET studies. For pathological diagnosis, he underwent CT-guided biopsy of primary lung cancer as well as ultrasound-guided biopsy of liver metastasis.

The immunohistochemical analyses, such as CK7, CK20 and TTF1, were consistent with lung adenocarcinoma (Figure 1B; positive for CK7 and TTF1, negative for CK20). In pathologic studies, his lung adenocarcinoma was negative for known *EGFR*, *KRAS* and *ALK* mutations (*EML4-ALK* fusion gene). The specimen from AK55 was referred to the Genomic Medicine Institute at Seoul National University (GMI-SNU) for identification of the driver mutations of the cancer by high-throughput analysis of whole-genome and transcriptome sequencing.

Results

Whole-genome analysis

From whole-genome deep sequencing of liver metastatic lung cancer tissue and normal tissue (blood) of AK55, we obtained 47.77x and 28.27x average read-depth, respectively (Table 1). The whole-genome coverage of liver metastatic lung cancer tissue was evenly distributed (excepting normal 'spikes' (Kim et al. 2009) of repetitive sequences in the centromeric or telomeric regions) suggesting no evidence of aneuploidy in the cancer tissue (Figure 2A). The bimodal distribution of read-allele frequency of single nucleotide variants (SNVs) on 0.5 and 1.0 also supports the euploidy of the genome of liver metastasis (Supplemental Figure 1). The whole-genome sequence of blood DNA demonstrated that AK55 does not have any remarkable cancer-related SNVs archived in OMIM (Online Mendelian Inheritance in Man) and SNPedia (http://www.snpedia.org), suggesting his lung cancer is unlikely to be driven by germline mutations. We identified 10,390 non-synonymous SNVs, 334 coding sequence (CDS) indels and 70 candidates of large deletion on CDS from the whole-genome sequences of liver metastasis (Supplemental Tables 1-3). Comparison of whole-genome sequences between liver metastatic cancer and normal tissue identified 10 non-synonymous somatic mutations (8 SNVs and 2 indels; Supplemental Tables 1-3 and Supplemental Figure 2). These 10 somatic mutations did not occur in genes with known driver mutations, such as *EGFR*, *KRAS*, *BRAF*, *PIK3CA*, *AKT1*, *MAP2K1* and *MET* (Pao and Girard 2011). Given the known functions of the genes affected by the somatic mutations and functional annotation of the 8 SNVs using the SIFT algorithm (Kumar et al. 2009), those somatic mutations are not thought to have a significant impact on lung cancer transformation. The somatic mutations may be present in the primary lung cancer or may have occurred during metastasis. In any case, we suggest they are unlikely to be driver mutations.

By comparison of DNA and RNA sequences, we examined A to I RNA editing in liver metastatic cancer tissues (Supplemental Table 4) (Shah et al. 2009; Ju et al. 2011). We found 10 RNA editing candidate sites in total, however, their functional impacts were not sufficient to be fundamental driver mutations of cancer.

Fusion gene analysis

Next, we analyzed transcriptome sequencing data from liver metastatic lung cancer. We focused on detecting fusion genes since not only hematologic but also solid cancers are known to be driven by fusion genes resulting from pathogenic chromosomal translocation or inversion (Tomlins et al. 2005; Wong et al. 2009; Tao et al. 2011; Welch et al. 2011). Our approaches identified 52 fusion genes (Figure 2A; Table 2; Supplemental Table 5; Supplemental Methods). Of these, 94.2% (n=49) were intrachromosomal fusions between adjacent genes (< 135 Kb), which may not have any functional roles in oncogenesis (Nacu et al. 2011) (Table 2). In addition, one (1.9%) was an inter-chromosomal fusion, but this was generated by haptoglobin (*HP*), which is highly expressed in liver. Although the existence of this fusion gene is interesting biologically, given the molecular function of the gene, it is not believed to have an impact on cellular transformation. The remaining two (3.8%) were *KIF5B-RET* and *KIAA1462-KIF5B* fusion genes, which were intrachromosomal fusions between remote genes (>~2Mb). Of these, *KIAA1462-KIF5B* was excluded, since its expression level is low and *KIAA1462* is a hypothetical protein of which the molecular function is not known. Out of the 52 fusion genes, we could detect a corresponding chromosomal rearrangement (e.g. large deletion, inversion or translocation) only in *KIF5B-RET* from the whole-genome sequence of liver metastatic lung cancer tissue (described later). To our knowledge, this fusion gene has not been reported in human cancer previously. The final gene fusion, *KIF5B-RET*, is interesting in particular since *RET* is a well known

tyrosine-kinase proto-oncogene (Takahashi et al. 1985). The name of *RET* originated from 'REarranged during Transfection', as the DNA sequence of this gene was discovered rearranged when discovered. Although RET is essential for development of the enteric nervous system and kidney in embryogenesis (Durbec et al. 1996), its expression level in normal lung tissue is generally very low (Su et al. 2002). However, chimeric forms of the *RET* oncogene with many kinds of partner genes are well known as driver mutations in papillary thyroid carcinoma (PTC) (Alberti et al. 2003). The molecular activation mechanism of chimeric RET tyrosine kinase with dimerization units of diverse partner genes are well understood in PTC. The dimerization unit stimulates autophosphorylation of the tyrosine kinase unit in the chimeric oncogene (Alberti et al. 2003). Interestingly, *KIF5B*, the fusion partner gene of *RET* in the cancer tissue of AK55, contains a dimerization unit (coiled-coil domain) which induces homo-dimerization (Score et al. 2006; Takeuchi et al. 2009; Daire and Pous 2011).

Therefore, we further confirmed the characteristics of this gene fusion event using the transcriptome sequencing data. The fusion transcript was highly expressed, as evidenced by 34 discordant paired-end reads and 60 spanning reads across the fusion-junction (Table 2 and Figure 2B). These data showed that the end of the 16th exon of *KIF5B* and the start of the 12th exon of the *RET* proto-oncogene (which is a rearrangement hotspot in RET fusion gene in PTCs, (Alberti et al. 2003)) were integrated. The fusion transcripts were validated using PCR amplification and Sanger sequencing of cDNA from liver metastatic lung cancer tissue (Figure 2C, 2D). In addition, the expression profile of *RET* showed that exons after fusion breakpoints (from 12th to 20th exon) are exclusively expressed (Figure 2E) in the liver metastatic lung cancer tissue, suggesting most of the *RET* expression in the cancer took place from the fusion gene rather than from the natural *RET* gene. The expression levels of these exons (exon 12 – 20) are approximately 10 times higher than those of lung cancers without *RET* rearrangement (Supplemental Table 6). In addition, given the genetic sequence, the fusion protein would contain both a dimerization unit (coiled-coil domain of KIF5B) and a

tyrosine kinase unit (from RET) (Figure 3A, 3B).

KIF5B and *RET* are 10.6 Mb away from each other, located at 10p11.22 and 10q11.21, respectively. Because the coding strands for the two genes are different, a 10.6 Mb-long inversion event is necessary for generating the fusion gene (Figure 4A). We confirmed this genomic inversion event in the liver metastatic lung cancer tissue by detecting highly confident reads supporting the inversion (8 reads). Considering the count of reads supporting normal chromosome structure (6 reads), we conclude that the *KIF5B-RET* fusion was present in the major subpopulation of liver metastatic lung cancer tissue (Supplemental Methods). In blood, however, there was no corresponding chromosomal rearrangement in the whole-genome sequencing. We found a single read suggesting the inversion in the whole-genome sequence from primary lung cancer, which alone is not sufficient to confirm the origin of this inversion. Hence, we validated the chromosomal inversion using PCR amplification and Sanger sequencing. DNA samples from three cancer tissues of AK55 (primary lung cancer, bone and liver metastatic lung cancer tissues), but not normal blood, showed PCR products resulting from the inversion event (Figure 4B). This confirms that the fusion gene also exists in the primary lung cancer as well as in bone metastatic cancer tissue. Sanger sequencing identified the breakpoints of the inversion with nucleotide resolution (chr10:32,351,306-42,931,601; Figure 4C). Interestingly, a single base-pair deletion was identified 2bp-adjacent to the breakpoint (chr10:42,931,604), suggesting an error-prone DNA repair mechanism, such as non-homologous end joining (NHEJ), fork stalling and template switching (FoSTeS) or microhomology-mediated break-induced replication (MMBIR), might have contributed to this inversion event after double-strand DNA breaks (Hastings et al. 2009; Zhang et al. 2009; Kee and D'Andrea 2010). Furthermore, the G-quadruplex (a non-B DNA) structure is predicted in the ~100 bp upstream of the rearrangement hotspot of *RET*, which is known to be fragile and a source of chromosomal rearrangements (Nambiar et al. 2011).

Recurrence of *KIF5B-RET* in primary lung adenocarcinomas

In order to show that the *KIF5B-RET* fusion gene also exists in other primary lung adenocarcinomas, we analyzed transcriptomes of 5 additional triple-negative (*EGFR*, *KRAS*, and *EML4-ALK*) primary lung adenocarcinomas using massively parallel sequencing (here we call them LC_S1 - S5; Supplemental Table 7). *KIF5B-RET* fusion transcripts were found in LC_S2. Like in AK55, *RET* was highly expressed from 12th exon (Supplemental Table 6). Because *KIF5B* is generally expressed in differentiated tissue (Su et al. 2002), the *KIF5B-RET* fusion gene could be expressed by the active promoter of *KIF5B* in those lung cancer tissues (AK55 and LC_S2). We validated this fusion transcript in LC_S2 using cDNA PCR (Figure 5A).

In addition, we further assessed the *KIF5B-RET* fusion gene using cDNA PCR of 15 more double-negative (*EGFR* and *EML4-ALK* were negative in pathologic studies; *KRAS* mutation status was unknown) primary lung adenocarcinomas (LC_S6 - S20). LC_S6 showed the *KIF5B-RET* fusion gene (Figure 5B). The breakpoint of the fusion gene in LC_S6 was identified using Sanger sequencing (Supplemental Figure 3). Overall, we identified two cases of the *KIF5B-RET* fusion gene (LC_S2 and LC_S6) in 20 primary lung adenocarcinomas in the replication study. These results clearly show that *KIF5B-RET* fusion is not rare and that the fusion transcript exists in the primary lung adenocarcinomas. In addition, because it would be very unlikely to find identical non-functional fusion genes in different cancer tissues, these results also provide indirect evidence that expression of the *KIF5B-RET* fusion gene has an important functional impact in lung cancer.

Interestingly in LC_S2 and LC_S6, exon 12 of *RET* was joined to exon 15 (LC_S2) and exon 23 (LC_S6) instead of to exon 16 of *KIF5B* as in AK55 (Figure 5C). These suggest that the double-strand breaks of DNA in *KIF5B* may not be consistent among primary lung cancers. However, because, their coiled-coil domains are well preserved in the KIF5B-RET chimeric

oncogene in both the samples (the length of coiled-coil domain in the fusion gene: 247 and 520 amino acids in LC_S2 and LC_S6, respectively), the dimerization activity is probably not very different compared with that of AK55 (310 amino acids).

Discussion

AK55 was referred for genetic study because of atypical features of his lung cancer: never-smoker, young age, multiple metastases, no family history and no known somatic mutations in conventional cancer marker tests in the clinic. Massively parallel DNA and RNA sequencing of cancer and normal tissues successfully identified the genetic cause of his lung adenocarcinoma. As sequencing technologies develop, whole-genome and transcriptome sequencing can be achieved within the time necessary for making therapeutic decisions. In addition, the cost of sequencing has been reducing dramatically in recent years. Now, human whole-genome deep sequencing analysis together with transcriptome analysis can be completed for under $10,000 within 3 weeks from tissue sampling. Given the fact that each cancer is transformed by its unique mutation events and this information is essential for medical therapeutic decisions, it is clear that cancer genome and transcriptome sequencing should be performed as a crucial cancer diagnostic procedure in the near future. This will especially benefit those patients whose cancer does not have any known cancer driver mutations.

Integration of genome and transcriptome sequencing has several remarkable advantages for identifying somatic cancer mutation. First, cross-checking of the results between DNA and RNA sequencing enables the extensive removal of false positives. Because the human genome consists of ~3 Gb, whole-genome sequencing generally includes thousands of false positive calls even though its accuracy is greater than 99.9999%. Second, transcriptome sequencing allows us to concentrate on specific genomic variants which are related to the genes under active transcription in the cancer. Cancer genomes may include hundreds of somatic passenger mutations. To isolate important driver mutations among them, we can use the information of expression levels in the cancer. Third, integration of DNA and RNA sequencing provides an opportunity to find variations generated during the gene

transcription process, such as RNA editing. Lastly, transcriptome sequencing can provide information of fusion genes generated by chromosomal inversion or translocation more easily than whole-genome sequencing. *Ab initio* detection of chromosomal rearrangements, such as translocation and inversion, is still challenging in whole-genome sequencing alone without specific targets. These difficulties can clearly be overcome by combining whole-genome and transcriptome sequencing.

The oncogenic effect of *RET* was first identified in papillary thyroid carcinoma (PTC) where diverse kinds of chromosomal translocations and inversions led to the formation of PTC/RET fusion genes (Alberti et al. 2003). Specific point mutations have also been reported as drivers in multiple endocrine neoplasia (MEN) types 2A and 2B (Alberti et al. 2003). In addition, activated *RET* has been observed in prostate cancer (Dawson et al. 1998), pancreatic cancer (Zeng et al. 2008) and melanoma (Ohshima et al. 2010). The direct transforming impact of *RET* as a driver is also supported by *RET* transgenic mice studies which generated a variety of malignancies (Portella et al. 1996; Kawai et al. 2000). However, this gene has not been highlighted in lung cancer previously.

Using the integrated sequencing technologies, we demonstrated a novel *KIF5B-RET* fusion gene in a lung adenocarcinoma for the first time. Although we found the fusion gene in a small number of samples, the evidence for its transforming role is convincing for the following reasons: (1) the fusion stands out based on direct data analysis from lung cancers not containing any known driver mutation; (2) RET is an established oncogene in other tumors; (3) the tyrosine kinase domain of RET is highly expressed exclusively in lung cancer samples containing the fusion gene; and (4) the partner gene (*KIF5B*) has the coiled-coil domain which is a well known dimerization unit and is necessary for activation of the fusion oncogene. Given the frequencies of known somatic mutations in lung adenocarcinoma, e.g. *EGFR* (~ 15%), *KRAS* (~ 25%) mutations, *EML4-ALK* fusion gene (~ 5%) and others (~15%) (Harris 2010; Pao and Girard 2011), a considerable number of unexplored mutations still remain to be identified (~ 40% of lung adenocarcinoma). Because we found two *KIF5B-RET*

fusions out of 20 primary lung adenocarcinomas (one of the five triple-negative (*EGFR*, *KRAS* and *EML4-ALK*) and one of the fifteen double-negative (*EGFR* and *EML4-ALK*)), we may estimate that the frequency of the fusion gene would be about ~ 6% in lung adenocarcinoma (4.3-8%; 1/5x40% = 8% from triple-negative cancers; 1/15 x 65% = 4.3% from double negative cancers). Interestingly, the Cancer Genome Atlas (TCGA) dataset showed *RET* overexpression in 3 out of 32 samples (9.4%; Supplemental Figure 4). Because sample size of our study is small (3 cases of the *KIF5B-RET* fusion gene in total of 21 samples) and there may be additional molecular mechanisms for *RET* overexpression (in TCGA dataset), such as negative mutants in the regulating domains of *RET*, genomic amplification, and *RET* fusion with other partner genes, further epidemiological studies are highly necessary to understand the frequency of the *KIF5B-RET* fusion with more accuracy.

In summary, we reported a novel *KIF5B-RET* fusion oncogene as a driver mutation of lung adenocarcinoma. This fusion gene may be a good therapeutic molecular target for treatments of lung cancer. Developments of specific agents targeting *KIF5B-RET* will provide more advanced therapeutic strategies for lung adenocarcinoma.

Methods

All protocols of this study were approved by the Institutional Review Board of Seoul St. Mary's Hospital (Approval # KC11OISI0603). In pathologic studies in the hospital (Seoul National University Hospital), mutations of *EGFR* and *KRAS*, and *EML4-ALK* fusion gene were examined from primary lung adenocarcinoma tissues. The results were all negative. Regarding *EGFR and KRAS*, nucleotide variations of exon 18-21 (*EGFR*) and exon 2 (*KRAS*) were studied using PCR and DNA sequencing as previously reported (Lynch et al. 2004; Eberhard et al. 2005). For *EML4-ALK*, fluorescence in situ hybridization study was performed as previously reported (Kwak et al. 2010).

We obtained paraffin-embedded tissues from primary lung cancer and bone metastasis. A frozen tissue from biopsy of liver metastasis was also available to use. In addition, we extracted venous blood of AK55. Genomic DNA was extracted from the lung cancer, bone metastasis, liver metastasis and blood. Furthermore, we extracted RNA from the frozen liver metastasis. Then cDNA was synthesized from total RNA as described previously (Ju et al. 2011). Sequencing libraries were generated according to the standard protocol of Illumina Inc. for high-throughput sequencing. Excluding the genomic DNA from paraffin-embedded bone metastasis (of which DNA concentration was too low for it to qualify under our criteria for generating the sequencing library), samples were sequenced using Illumina HiSeq2000 and Genome Analyzer IIx (Table 1). Because the DNA of primary lung cancer was extracted from a small amount of DNA in the paraffin-embedded tissue, the short-read redundancy was too high for analysis. Hence, our primary comparisons were done between the sequences from liver metastasis and blood. The sequencing experiments were performed using the standard methods of Illumina and our previous reports (Kim et al. 2009; Ju et al. 2011)

For replication study, we obtained 5 more frozen primary lung adenocarcinoma tissues (LC_S1 – S5) which were determined to be *EGFR*, *KRAS* and *EML4-ALK* negative in the

pathologic studies mentioned above. We sequenced the transcriptome (cDNA from whole mRNA) using Illumina Hiseq2000 as described above. In addition, we also obtained 15 frozen primary lung adenocarcinoma tissues (LC_S6 - S20) from patients negative for *EGFR* and *EML4-ALK*, but whose *KRAS* status was unknown (these 15 samples were assessed using PCR and Sanger sequencing as described below).

Short reads were aligned to the NCBI reference human genome assembly (build 36.3, hg18) using the GSNAP (Wu and Nacu 2010) alignment program, with allowance for 5% mismatches. We called genomic variants of each sample, e.g. single nucleotide variation (SNV), short insertion and deletion (indel) and large deletions, using modified criteria from our previous publications in whole-genome sequencing (Kim et al. 2009; Ju et al. 2011). Briefly, SNVs and indels were defined based on satisfaction of the following three conditions: (1) the number of uniquely mapped reads at the position should be ≥2; (2) the average base quality (Phred Q score) for the position should be eho; (3) the read-allele frequency at the position should be eoul. For detection of somatic mutations (SNVs and indels) in liver metastatic lung cancer tissues, we used the following conditions: (1) non-synonymous SNVs or indels in liver metastatic lung cancer tissues; (2) the SNV allele count should be zero in whole-genome sequence of blood; (3) the wildtype allele count should be ≥10 in whole-genome sequence of blood; and (4) the candidate positions should not be detected in Korean genomes (Ju et al. 2011) and 1000 Genomes Project (Durbin et al. 2010). Large deletion candidates on CDS were identified using modified criteria from our previous publications in whole-genome sequencing (Ju et al. 2011). Briefly, (1) there should be ≥2 long-insert paired-end reads; (2) sequencing read-depth of large deletion candidate region should be < 90% of that of its flanking regions; (3) size of large deletion ≥200 bp. To detect large deletions caused by somatic mutation, we visually compared the read-depth between whole-genome sequence of liver metastatic lung cancer and blood tissue (Supplemental Figure 2). For identifying RNA editing in liver metastatic lung cancer tissue, we used more

conservative criteria than those used previously (Ju et al. 2011), since we have only a pair of DNA and RNA sequencing data of lung cancer (liver metastasis) and hence comparison of many samples was impossible. Our criteria were (1) clear non-synonymous A to G SNVs (in coding strand) in transcriptome sequencing with ≥10 high quality (Phred Q score ≥25) mismatches, read-allele frequency ≥20%; (2) clear wildtype in genome sequencing (count for SNVs allele =0, count for wildtype ≥ 10; (3) not located on repetitive genomic regions.

RNA sequencing data was also analyzed as described previously (Ju et al. 2011). Using the GSNAP alignment tool (Wu and Nacu 2010), we aligned short reads from transcriptome sequencing to a set of constructed mRNA sequences instead of the reference human genome to avoid mapping errors resulting from mRNA splicing (Ju et al. 2011). We allowed 5% mismatches for the alignment. The expression profiles were calculated using the RPKM unit as described (Mortazavi et al. 2008). For SNV detection in transcriptome sequencing (for RNA editing), 15 bp of both ends of a read were trimmed and not used, since end sequences are easily misaligned (mostly due to alternative splicing of transcripts).

For detection of fusion genes using transcriptome sequencing, we used discordant read pairs, where the reads of a pair were aligned to different genes, and exon-spanning reads across the fusion breakpoint of chimeric transcripts. Because there can be a lot of false positives in the massively parallel sequencing reads, we further applied three filter criteria as follows: (1) the homology filter; (2) the fusion-spanning read filter; and (3) the fusion point filter. We described the details of methods for identifying fusion genes in Supplemental Methods. Regarding final fusion gene candidates, we assessed corresponding genomic rearrangements, such as inversions, translocations and large deletions in the whole-genome sequencing data.

We validated our findings using PCR amplification and Sanger sequencing of genomic DNA and cDNA. The PCR reactions were at 95 ℃ for 10 min, 30 cycles of 95 ℃ for 30 s, 62 ℃ for 10s 72 ℃ for 10 s and, finally, 72 ℃ for 10 min. PCR and Sanger sequencing primers for

genomic inversion of AK55 were 5'- CAGAATTTCACAAGGAGGGAAG-3' (*KIF5B*) and 5'-CAGGACCTCTGACTACAGTGGA-3' (*RET*). Primers for fusion transcripts are 5'-GTGAAACGTTGCAAGCAGTTAG-3' (*KIF5B*) and 5'-CCTTGACCACTTTTCCAAATTC-3' (*RET*). For cDNA PCR in replication studies, we used different *KIF5B* primers (5'-TAAGGAAATGACCAACCACCAG-3') since the *KIF5B* fusion breakpoint in LC_S2 was different to that in AK55. All the Sanger sequencing experiments were performed at Macrogen Inc. (http://www.macrogen.com).

Data access

Sequencing reads are uploaded in EBI-SRA under accession number ERP001071 (whole-genome sequencing; http://www.ebi.ac.uk/ena/data/view/ERP001071) and ERP001058 (transcriptome sequencing; http://www.ebi.ac.uk/ena/data/view/ERP001058). The short-read data are also available from the authors' website (ftp://ftp.gmi.ac.kr/asianGenome/AK55/, http://tiara.gmi.ac.kr/). The program developed and used for detecting fusion genes in this study (GFP; Gene Fusion Program) is also available from ftp://ftp.gmi.ac.kr/pub/GFP/.

Acknowledgments

We are grateful to the lung cancer patients who participated in this study and provided their cancer tissues for medical research. We are indebted to the scientists and medical doctors who contributed to this work but were not included in the author list. We thank The Cancer Genome Atlas (TCGA) Project Team and their specimen donors for providing expression profile data. This work has been supported by Macrogen Inc. (MG2011009). The authors declare no competing financial interests.

Figure Legends

Figure 1. Pathology of lung adenocarcinoma analyzed in this study

(A) A paraffin section stained by hematoxylin and eosin from a primary lung cancer tissue obtained by CT-guided biopsy (x400). In the cancer tissue, poorly differentiated tumor cell nests were present in the desmoplastic stroma. In addition, the cancer cells had plump cytoplasm and large pleomorphic nuclei.

(B) Immunohistochemical analyses of the cancer (from metastatic tumor in the cervical spine). From left to right, CK7 (positive), TTF1 (positive) and CK20 (negative). The results highly suggest that the origin of this cancer is lung adenocarcinoma.

Figure 2. Discovery of novel transforming *KIF5B-RET* fusion gene in lung adenocarcinoma.

(A) Graphical representation of whole-genome and transcriptome sequencing data from the liver metastatic lung cancer tissue. Chromosome ideograms are shown in the outer layer. Coverage of cancer whole-genome sequencing is shown in the 1st middle layer. Expression level of genes is shown in the 2nd middle layer using heatmap. Intra- and interchromosomal fusion genes are shown in the central layer. The thickness of lines shows the amount of evidence (number of spanning reads). The *KIF5B-RET* fusion gene is shown in red.

(B) Detection of *KIF5B-RET* fusion gene from transcriptome sequencing. We identified 34 ‘discordant paired-end reads’ and 60 ‘spanning reads’ across the exon-junction. A discordant paired-end read is defined as a read whose end-sequences are aligned to each of the fusion partner genes. A spanning read is a read, one of whose end-sequences is aligned across the junction of the predicted fusion transcript. In this analysis, the fusion occurred between the 16th exon of *KIF5B* and 12th exon of *RET*.

(C) Validation of *KIF5B-RET* fusion transcript in RNA (cDNA) from liver metastatic cancer tissue by PCR amplification and electrophoresis. The fusion gene is only

detected in the liver metastatic lung cancer tissue of AK55. The negative control cDNA (normal) were extracted from a blood of healthy Korean individual (AK1) (Kim et al. 2009)

(D) Validation of the fusion gene breakpoint using Sanger sequencing in cDNA

(E) RNA expression level of each *RET* exon. Active expression is observed from the 12th exon, downstream of the junction of predicted *KIF5B-RET* fusion gene. This suggests that the *RET* oncogene is expressed exclusively from the fusion gene, rather than natural *RET* gene.

Figure 3. Molecular characteristics of KIF5B-RET fusion kinase.

(A) Functional domains of KIF5B-RET fusion kinase. The fusion kinase consists of 638 N-terminal residues of KIF5B and 402 C-terminal residues of RET kinase. As a result, the fusion protein consists of a protein kinase domain together with a coiled-coil domain. The coiled-coil domain induces dimerization of the fusion kinase, which activates the oncogenic protein tyrosine kinase domain by autophosphorylation.

(B) Three dimensional structure of the KIF5B-RET chimeric oncogene, as predicted by the PHYRE2 algorithm (Kelley and Sternberg 2009). The N- and C-terminal of the fusion protein are colored in red and blue, respectively.

Figure 4. A chromosomal rearrangement for generating *KIF5B-RET* fusion in the lung cancer tissue of AK55.

(A) Detection of a 10.6 Mb-long inversion event in chromosome 10 from the whole-genome sequencing of the liver metastatic lung cancer. *KIF5B* is generally expressed with its universal promoter. By the inversion event, this promoter activates global expression of the *KIF5B-RET* fusion gene.

(B) Validation of *KIF5B-RET* fusion gene DNA by inversion-specific PCR amplification and electrophoresis. The fusion gene is only detected in the cancer tissues of AK55 (primary lung cancer, liver and bone metastatic lung cancer tissues). The negative control DNA sample were extracted from a healthy Korean individual (AK1) (Kim et al. 2009)

(C) Identification of the fusion gene and inversion breakpoint using Sanger sequencing. The inversion breakpoints were located in the introns of *KIF5B* and *RET* as predicted. Two bases downstream from the breakpoint (chr10:42,931,604, hg18), a 1 bp deletion was identified, suggesting error-prone DNA repair mechanisms might contribute to this inversion event after double-strand DNA breaks.

Figure 5. Replication studies of *KIF5B-RET* fusion gene in an additional five triple-negative lung adenocarcinomas.

(A) cDNA PCR targeting *KIF5B-RET* fusion transcripts and gel electrophoresis in liver metastatic lung cancer of AK55 and 5 additional triple-negative lung adenocarcinomas. cDNA from AK55 and LC_S2 shows clear evidence of the fusion transcript. Because the fusion transcript in AK55 contains one more exon of *KIF5B* (exon 16) compared with that in LC_S2 (exon 15), the size of PCR product in AK55 is longer than that in LC_S2.

(B) cDNA PCR targeting *KIF5B-RET* fusion transcripts and gel electrophoresis in 15 double-negative lung adenocarcinomas. LC_S6 shows clear evidence of the fusion transcript. The fusion transcript in LC_S6 contains seven more exons of *KIF5B* (exon 17 - 23) compared with that in AK55.

(C) Comparison of schematic *KIF5B-RET* fusion transcripts between AK55, LC_S2 and LC_S6. Each rectangle indicates an exon of *KIF5B* (blue) and *RET* (red) gene.

Tables

Table 1. Summary statistics of sequencing analysis of the lung cancer patient AK55

Analysis	Tissue	Source	Massively Parallel Sequencing (mappable)				Validation
			Number of aligned reads	Read length (bp)	Through put (Gbp)	Read depth (fold)	PCR and Sanger sequencing
Genome							
	Blood	Fresh	392,194,564	2x103	80.79	28.27x	Yes
	Lung cancer*	Paraffin-embedded	274,909,815	2x103	56.63	19.81x	Yes
	Liver metastasis	Frozen	655,670,934	2x101, 2x108	136.55	47.77x	Yes
	Bone metastasis	Paraffin-embedded	-	-	-	-	Yes
Transcriptome							
	Liver metastasis	Frozen	89,682,934	101, 68	15.16	-	Yes

* Genome sequence of primary lung cancer was used only in the validation phase since the quality of DNA from FFPE was not sufficient for the discovery phase

Table 2. Selected fusion genes (20 out of 52 total) identified in the liver metastatic lung cancer of AK55.

Category	Donor gene	Acceptor gene	Chr	Distance (Mb)	# of discordant reads	# of spanning reads	Evidence in whole-genome sequence
Intra-chromosomal							
	KIF5B	*RET*	10	10.580	34	60	YES (inversion)
	KIF5B	*KIAA1462*	10	1.970	4	4	-
	EEF1DP3	*FRY*	13	0.133	3	5	-
	RPS6KB1	*TMEM49*	17	0.097	4	31	-
	HACL1	*COLQ*	3	0.075	3	4	-
	TMEM56	*RWDD3*	1	0.073	4	11	-
	FAM18B2	*CDRT4*	17	0.065	4	29	-
	CTBS	*GNG5*	1	0.065	6	27	-
	METTL10	*FAM53B*	10	0.054	2	4	-
	AZGP1	*GJC3*	7	0.048	5	15	-
	NKX2-1	*SFTA3*	14	0.046	3	7	-
	ADSL	*SGSM3*	22	0.036	5	6	-
	ART4	*C12orf69*	12	0.034	3	4	-
	LOC100131434	*IDS*	X	0.031	2	11	-
	LOC100130093	*SNAP47*	1	0.030	2	2	-
	C15orf57	*MRPL42P5*	15	0.025	2	7	-
	MIA2	*CTAGE5*	14	0.024	30	102	-
	SH3D20	*ARHGAP27*	17	0.024	2	10	-
	RBM14	*RBM4*	11	0.023	16	24	-
Inter-chromosomal	*RSPO1*	*HP*	16;1	-	2	3	-

References

Alberti L, Carniti C, Miranda C, Roccato E, Pierotti MA. 2003. RET and NTRK1 proto-oncogenes in human diseases. *J Cell Physiol* **195**(2): 168-186.

Daire V, Pous C. 2011. Kinesins and protein kinases: key players in the regulation of microtubule dynamics and organization. *Arch Biochem Biophys* **510**(2): 83-92.

Dawson DM, Lawrence EG, MacLennan GT, Amini SB, Kung HJ, Robinson D, Resnick MI, Kursh ED, Pretlow TP, Pretlow TG. 1998. Altered expression of RET proto-oncogene product in prostatic intraepithelial neoplasia and prostate cancer. *J Natl Cancer Inst* **90**(7): 519-523.

Durbec P, Marcos-Gutierrez CV, Kilkenny C, Grigoriou M, Wartiowaara K, Suvanto P, Smith D, Ponder B, Costantini F, Saarma M et al. 1996. GDNF signalling through the Ret receptor tyrosine kinase. *Nature* **381**(6585): 789-793.

Durbin R, Altshuler D, Abecasis G, Bentley D, Chakravarti A, Clark A, Collins FS, De La Vaga F, Donnelly P, Egholm M et al. 2010. A map of human genome variation from population-scale sequencing. *Nature* **467**(7319): 1061-1073.

Eberhard DA, Johnson BE, Amler LC, Goddard AD, Heldens SL, Herbst RS, Ince WL, Janne PA, Januario T, Johnson DH et al. 2005. Mutations in the epidermal growth factor receptor and in KRAS are predictive and prognostic indicators in patients with non-small-cell lung cancer treated with chemotherapy alone and in combination with erlotinib. *J Clin Oncol* **23**(25): 5900-5909.

Ferlay J, Shin HR, Bray F, Forman D, Mathers C, Parkin DM. 2010. Estimates of worldwide burden of cancer in 2008: GLOBOCAN 2008. *Int J Cancer*.

Harris T. 2010. Does large scale DNA sequencing of patient and tumor DNA yet provide clinically actionable information? *Discov Med* **10**(51): 144-150.

Hastings PJ, Ira G, Lupski JR. 2009. A microhomology-mediated break-induced replication model for the origin of human copy number variation. *PLoS Genet* **5**(1): e1000327.

Ju YS, Kim JI, Kim S, Hong D, Park H, Shin JY, Lee S, Lee WC, Yu SB, Park SS et al. 2011. Extensive genomic and transcriptional diversity identified through massively parallel DNA and RNA sequencing of eighteen Korean individuals. *Nat Genet* **43**(8): 745-752.

Kawai K, Iwashita T, Murakami H, Hiraiwa N, Yoshiki A, Kusakabe M, Ono K, Iida K, Nakayama A, Takahashi M. 2000. Tissue-specific carcinogenesis in transgenic mice expressing the RET proto-oncogene with a multiple endocrine neoplasia type 2A mutation. *Cancer Res* **60**(18): 5254-5260.

Kee Y, D'Andrea AD. 2010. Expanded roles of the Fanconi anemia pathway in preserving genomic stability. *Genes Dev* **24**(16): 1680-1694.

Kelley LA, Sternberg MJ. 2009. Protein structure prediction on the Web: a case study using the Phyre server. *Nat Protoc* **4**(3): 363-371.

Kim JI, Ju YS, Park H, Kim S, Lee S, Yi JH, Mudge J, Miller NA, Hong D, Bell CJ et al. 2009. A highly

annotated whole-genome sequence of a Korean individual. *Nature* **460**(7258): 1011-1015.

Kumar P, Henikoff S, Ng PC. 2009. Predicting the effects of coding non-synonymous variants on protein function using the SIFT algorithm. *Nat Protoc* **4**(7): 1073-1081.

Kwak EL, Bang YJ, Camidge DR, Shaw AT, Solomon B, Maki RG, Ou SH, Dezube BJ, Janne PA, Costa DB et al. 2010. Anaplastic lymphoma kinase inhibition in non-small-cell lung cancer. *N Engl J Med* **363**(18): 1693-1703.

Lee YJ, Kim JH, Kim SK, Ha SJ, Mok TS, Mitsudomi T, Cho BC. 2011. Lung cancer in never smokers: change of a mindset in the molecular era. *Lung Cancer* **72**(1): 9-15.

Lynch TJ, Bell DW, Sordella R, Gurubhagavatula S, Okimoto RA, Brannigan BW, Harris PL, Haserlat SM, Supko JG, Haluska FG et al. 2004. Activating mutations in the epidermal growth factor receptor underlying responsiveness of non-small-cell lung cancer to gefitinib. *N Engl J Med* **350**(21): 2129-2139.

Mortazavi A, Williams BA, McCue K, Schaeffer L, Wold B. 2008. Mapping and quantifying mammalian transcriptomes by RNA-Seq. *Nat Methods* **5**(7): 621-628.

Nacu S, Yuan W, Kan Z, Bhatt D, Rivers CS, Stinson J, Peters BA, Modrusan Z, Jung K, Seshagiri S et al. 2011. Deep RNA sequencing analysis of readthrough gene fusions in human prostate adenocarcinoma and reference samples. *BMC Med Genomics* **4**: 11.

Nambiar M, Goldsmith G, Moorthy BT, Lieber MR, Joshi MV, Choudhary B, Hosur RV, Raghavan SC. 2011. Formation of a G-quadruplex at the BCL2 major breakpoint region of the t(14;18) translocation in follicular lymphoma. *Nucleic Acids Res* **39**(3): 936-948.

Ohshima Y, Yajima I, Takeda K, Iida M, Kumasaka M, Matsumoto Y, Kato M. 2010. c-RET molecule in malignant melanoma from oncogenic RET-carrying transgenic mice and human cell lines. *PLoS One* **5**(4): e10279.

Paez JG, Janne PA, Lee JC, Tracy S, Greulich H, Gabriel S, Herman P, Kaye FJ, Lindeman N, Boggon TJ et al. 2004. EGFR mutations in lung cancer: correlation with clinical response to gefitinib therapy. *Science* **304**(5676): 1497-1500.

Pao W, Girard N. 2011. New driver mutations in non-small-cell lung cancer. *Lancet Oncol* **12**(2): 175-180.

Portella G, Salvatore D, Botti G, Cerrato A, Zhang L, Mineo A, Chiappetta G, Santelli G, Pozzi L, Vecchio G et al. 1996. Development of mammary and cutaneous gland tumors in transgenic mice carrying the RET/PTC1 oncogene. *Oncogene* **13**(9): 2021-2026.

Riely GJ, Kris MG, Rosenbaum D, Marks J, Li A, Chitale DA, Nafa K, Riedel ER, Hsu M, Pao W et al. 2008. Frequency and distinctive spectrum of KRAS mutations in never smokers with lung adenocarcinoma. *Clin Cancer Res* **14**(18): 5731-5734.

Schiller JH, Harrington D, Belani CP, Langer C, Sandler A, Krook J, Zhu J, Johnson DH. 2002. Comparison of four chemotherapy regimens for advanced non-small-cell lung cancer. *N Engl J Med* **346**(2): 92-98.

Score J, Curtis C, Waghorn K, Stalder M, Jotterand M, Grand FH, Cross NC. 2006. Identification of a

novel imatinib responsive KIF5B-PDGFRA fusion gene following screening for PDGFRA overexpression in patients with hypereosinophilia. *Leukemia* **20**(5): 827-832.

Shah SP, Morin RD, Khattra J, Prentice L, Pugh T, Burleigh A, Delaney A, Gelmon K, Guliany R, Senz J et al. 2009. Mutational evolution in a lobular breast tumour profiled at single nucleotide resolution. *Nature* **461**(7265): 809-813.

Soda M, Choi YL, Enomoto M, Takada S, Yamashita Y, Ishikawa S, Fujiwara S, Watanabe H, Kurashina K, Hatanaka H et al. 2007. Identification of the transforming EML4-ALK fusion gene in non-small-cell lung cancer. *Nature* **448**(7153): 561-566.

Su AI, Cooke MP, Ching KA, Hakak Y, Walker JR, Wiltshire T, Orth AP, Vega RG, Sapinoso LM, Moqrich A et al. 2002. Large-scale analysis of the human and mouse transcriptomes. *Proc Natl Acad Sci U S A* **99**(7): 4465-4470.

Subramanian J, Govindan R. 2007. Lung cancer in never smokers: a review. *J Clin Oncol* **25**(5): 561-570.

Takahashi M, Ritz J, Cooper GM. 1985. Activation of a novel human transforming gene, ret, by DNA rearrangement. *Cell* **42**(2): 581-588.

Takeuchi K, Choi YL, Togashi Y, Soda M, Hatano S, Inamura K, Takada S, Ueno T, Yamashita Y, Satoh Y et al. 2009. KIF5B-ALK, a novel fusion oncokinase identified by an immunohistochemistry-based diagnostic system for ALK-positive lung cancer. *Clin Cancer Res* **15**(9): 3143-3149.

Tao J, Deng NT, Ramnarayanan K, Huang B, Oh HK, Leong SH, Lim SS, Tan IB, Ooi CH, Wu J et al. 2011. CD44-SLC1A2 gene fusions in gastric cancer. *Sci Transl Med* **3**(77): 77ra30.

Toh CK, Gao F, Lim WT, Leong SS, Fong KW, Yap SP, Hsu AA, Eng P, Koong HN, Thirugnanam A et al. 2006. Never-smokers with lung cancer: epidemiologic evidence of a distinct disease entity. *J Clin Oncol* **24**(15): 2245-2251.

Tomlins SA, Rhodes DR, Perner S, Dhanasekaran SM, Mehra R, Sun XW, Varambally S, Cao X, Tchinda J, Kuefer R et al. 2005. Recurrent fusion of TMPRSS2 and ETS transcription factor genes in prostate cancer. *Science* **310**(5748): 644-648.

Welch JS, Westervelt P, Ding L, Larson DE, Klco JM, Kulkarni S, Wallis J, Chen K, Payton JE, Fulton RS et al. 2011. Use of whole-genome sequencing to diagnose a cryptic fusion oncogene. *JAMA* **305**(15): 1577-1584.

Wong DW, Leung EL, So KK, Tam IY, Sihoe AD, Cheng LC, Ho KK, Au JS, Chung LP, Pik Wong M. 2009. The EML4-ALK fusion gene is involved in various histologic types of lung cancers from nonsmokers with wild-type EGFR and KRAS. *Cancer* **115**(8): 1723-1733.

Wu TD, Nacu S. 2010. Fast and SNP-tolerant detection of complex variants and splicing in short reads. *Bioinformatics* **26**(7): 873-881.

Zeng Q, Cheng Y, Zhu Q, Yu Z, Wu X, Huang K, Zhou M, Han S, Zhang Q. 2008. The relationship between overexpression of glial cell-derived neurotrophic factor and its RET receptor with progression and prognosis of human pancreatic cancer. *J Int Med Res* **36**(4): 656-664.

Zhang F, Carvalho CM, Lupski JR. 2009. Complex human chromosomal and genomic rearrangements. *Trends Genet* **25**(7): 298-307.

Figure 1.

A

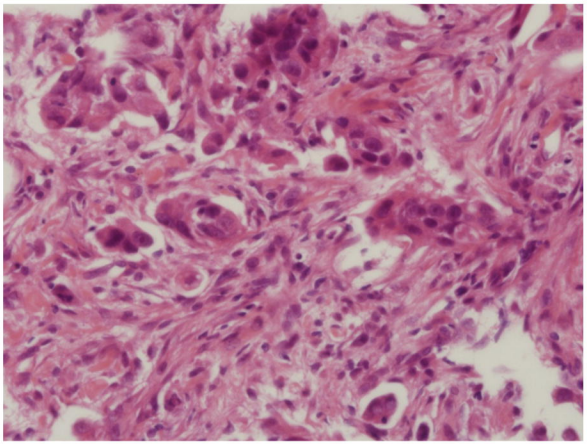

B

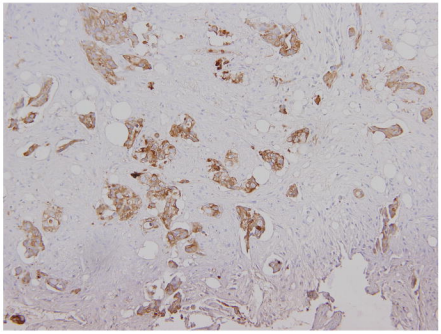

CK7 positive

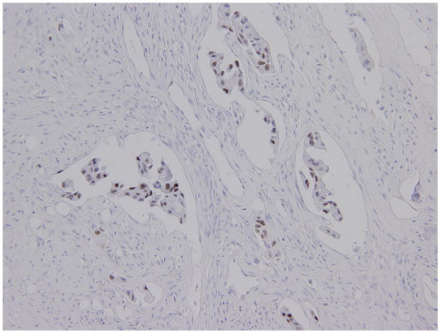

TTF1 positive

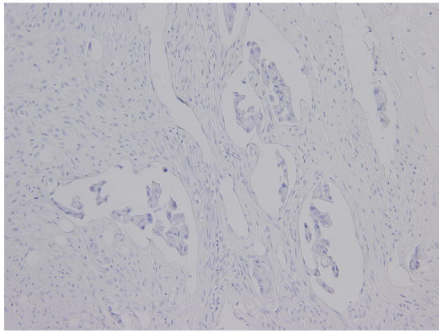

CK20 negative

Figure 2

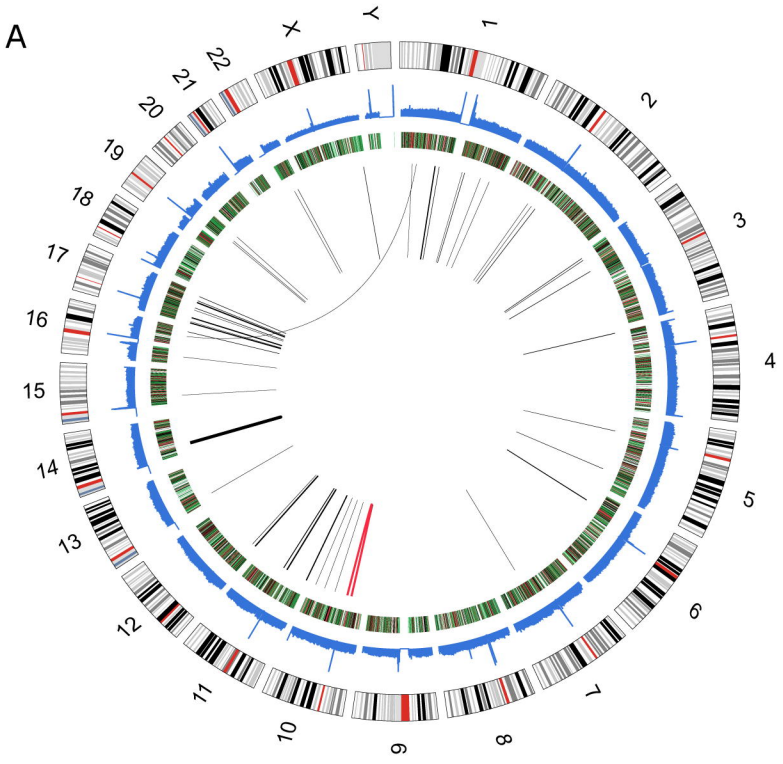
A
X
Y
1
2
3
4
5
6
7
8
9
10
11
12
13
14
15
16
17
18
19
20
21
22

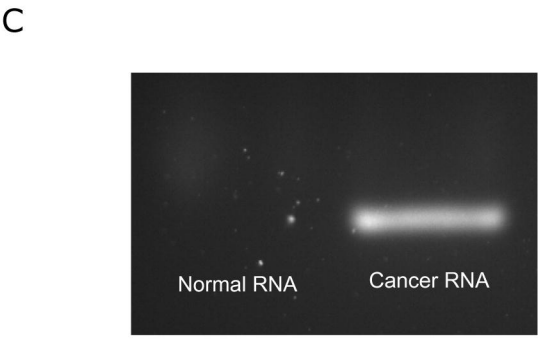
C
Normal RNA
Cancer RNA

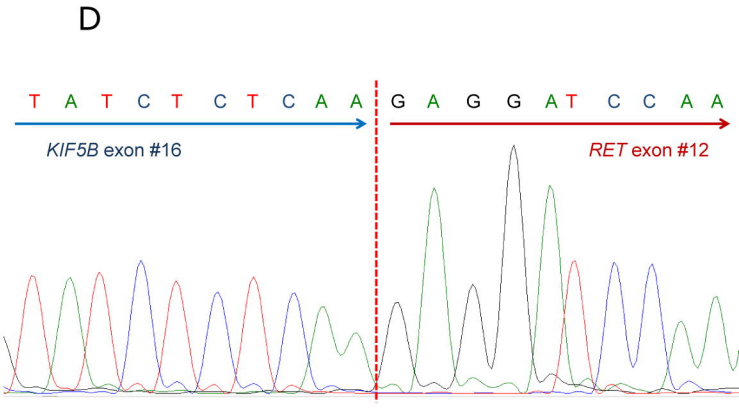
D
T A T C T C T C A A G A G G A T C C A A
KIF5B exon #16
RET exon #12

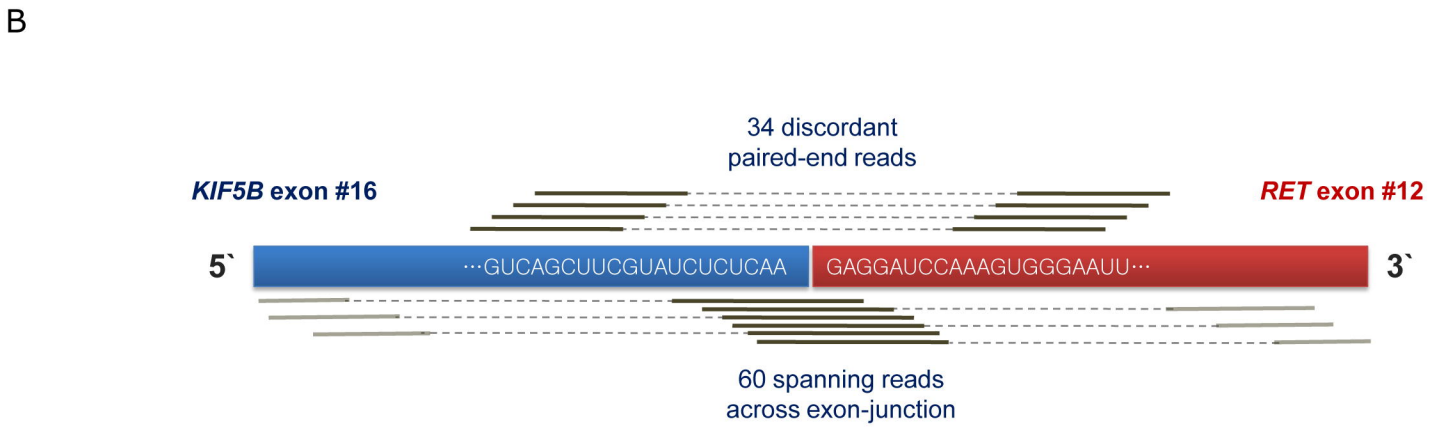
B
34 discordant
paired-end reads
KIF5B exon #16
RET exon #12
5`
···GUCAGCUUCGUAUCUCUCAA
GAGGAUCCAAAGUGGGAAUU···
3`
60 spanning reads
across exon-junction

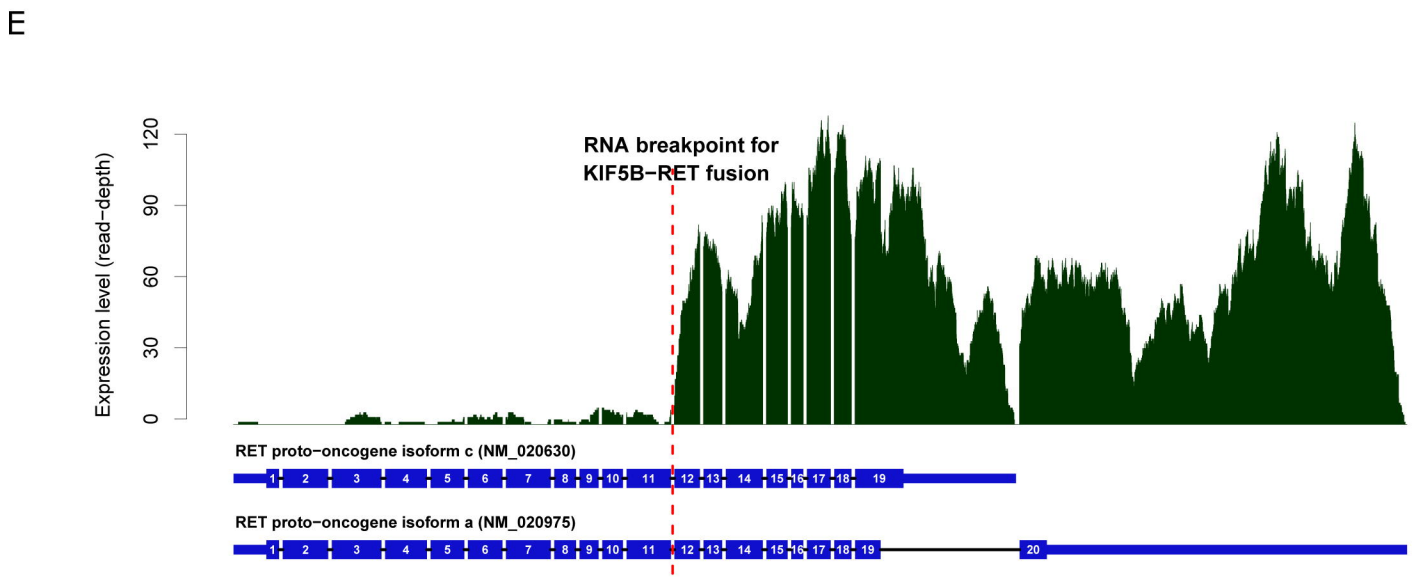
E
Expression level (read-depth)
0
30
60
90
120
RNA breakpoint for
KIF5B–RET fusion
RET proto-oncogene isoform c (NM_020630)
1 2 3 4 5 6 7 8 9 10 11 12 13 14 15 16 17 18 19
RET proto-oncogene isoform a (NM_020975)
1 2 3 4 5 6 7 8 9 10 11 12 13 14 15 16 17 18 19 20

Figure 3

A

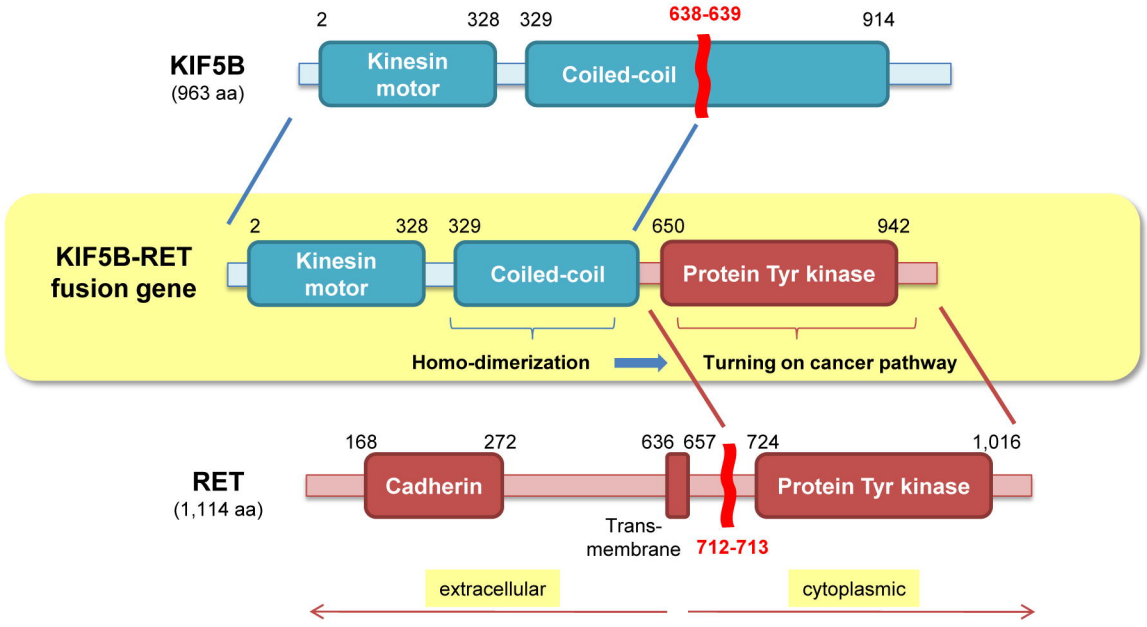
KIF5B
(963 aa)
2
328
329
638-639
914
Kinesin motor
Coiled-coil
KIF5B-RET fusion gene
2
328
329
650
942
Kinesin motor
Coiled-coil
Protein Tyr kinase
Homo-dimerization
Turning on cancer pathway
RET
(1,114 aa)
168
272
636
657
724
1,016
Cadherin
Protein Tyr kinase
Trans-membrane
712-713
extracellular
cytoplasmic

B

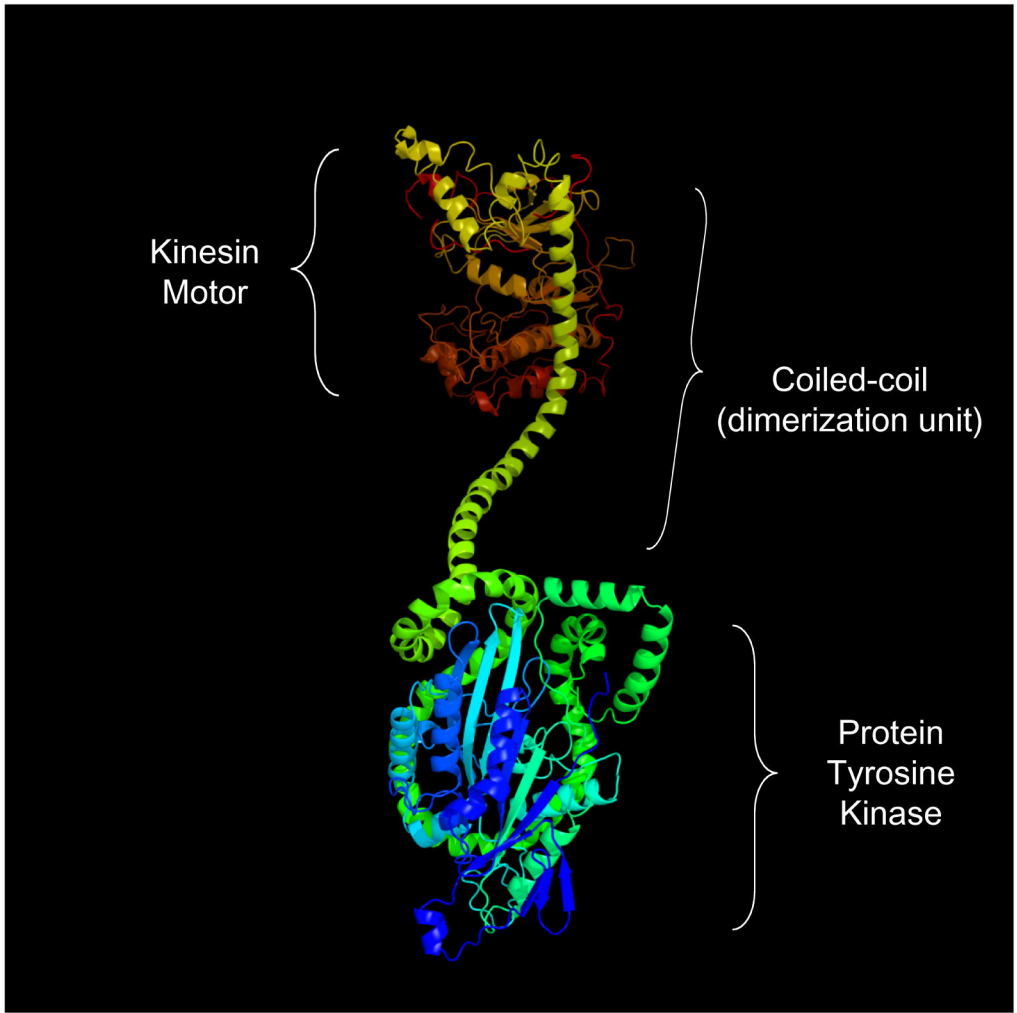
Kinesin Motor
Coiled-coil (dimerization unit)
Protein Tyrosine Kinase

Figure 4

A

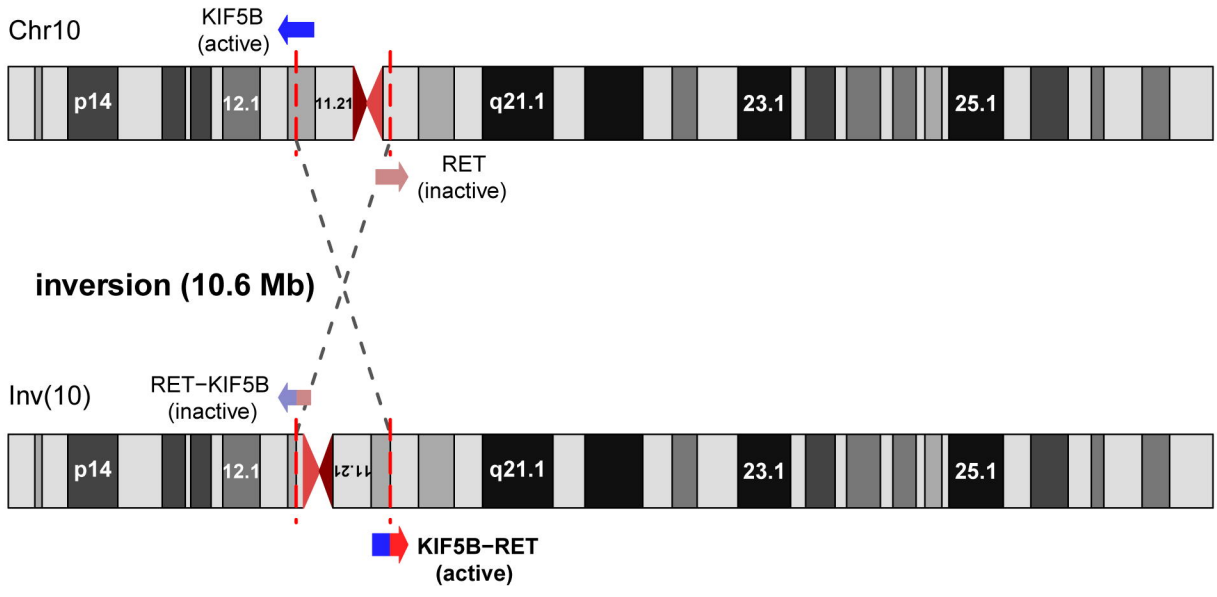
Chr10
KIF5B
(active)
p14
12.1
11.21
q21.1
23.1
25.1
RET
(inactive)
inversion (10.6 Mb)
Inv(10)
RET−KIF5B
(inactive)
p14
12.1
11.21
q21.1
23.1
25.1
KIF5B−RET
(active)

B

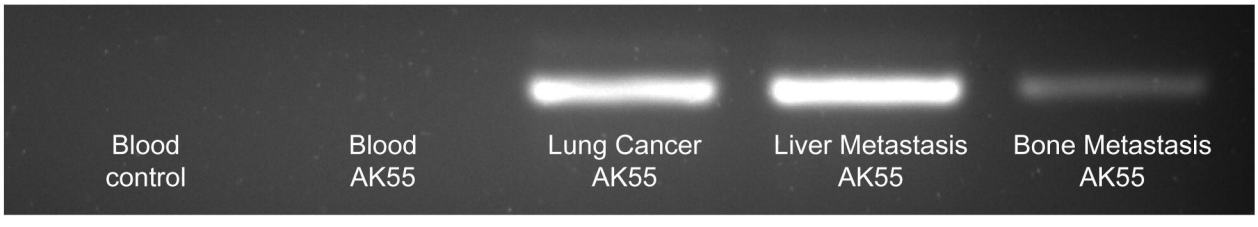
Blood
control
Blood
AK55
Lung Cancer
AK55
Liver Metastasis
AK55
Bone Metastasis
AK55

C

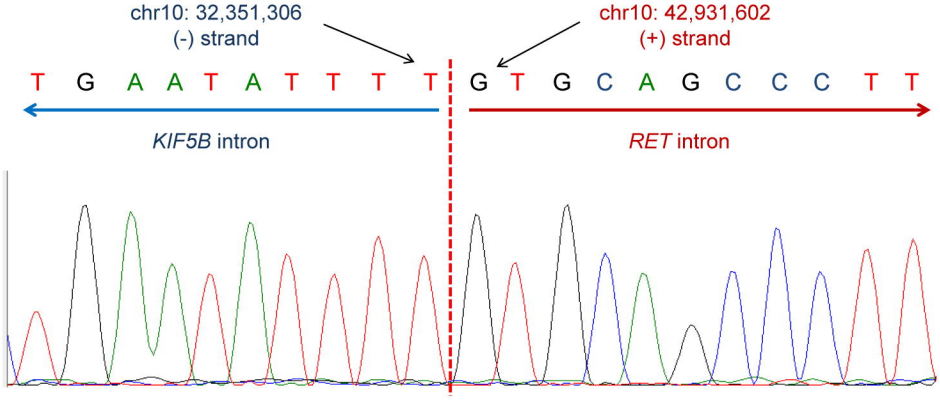
chr10: 32,351,306
(-) strand
chr10: 42,931,602
(+) strand
T G A A T A T T T T
G T G C A G C C C T T
KIF5B intron
RET intron

Figure 5

A

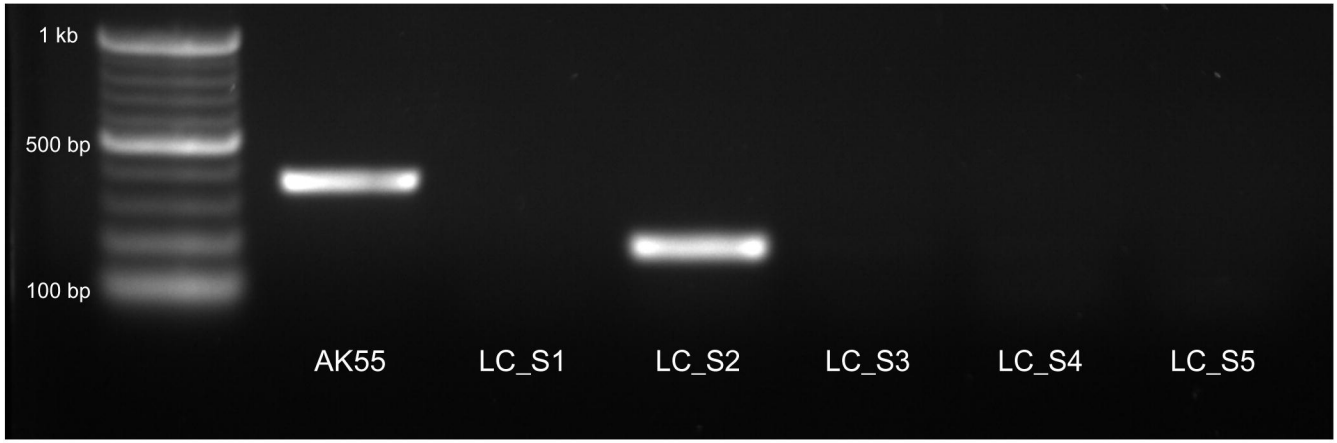
1 kb
500 bp
100 bp
AK55
LC_S1
LC_S2
LC_S3
LC_S4
LC_S5

B

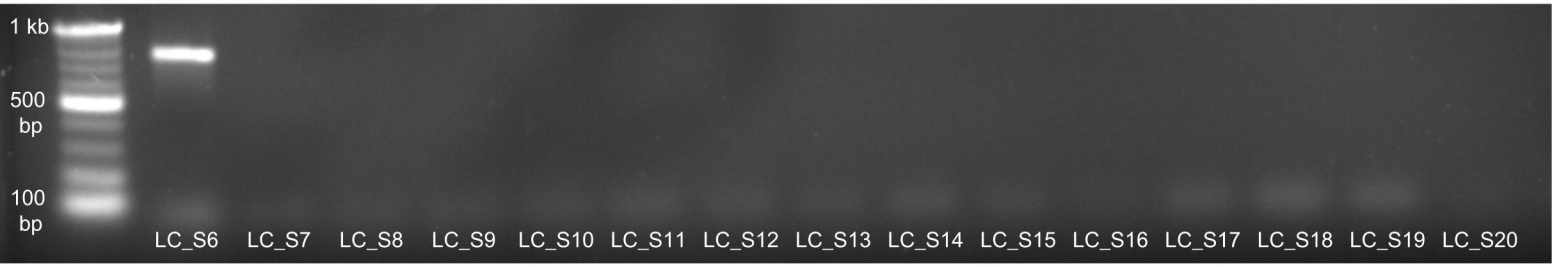
1 kb
500 bp
100 bp
LC_S6
LC_S7
LC_S8
LC_S9
LC_S10
LC_S11
LC_S12
LC_S13
LC_S14
LC_S15
LC_S16
LC_S17
LC_S18
LC_S19
LC_S20

C

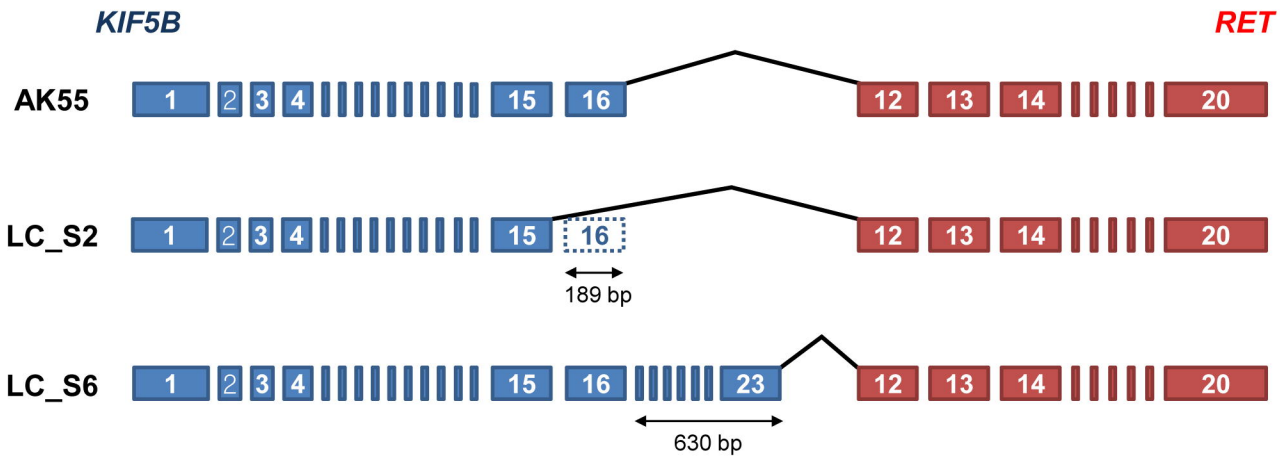
KIF5B
RET
AK55
LC_S2
LC_S6
1
2
3
4
15
16
23
12
13
14
20
189 bp
630 bp